

## Self-veto approaches to reject atmospheric neutrinos in KM3NeT/ARCA

---

**Thomas Heid<sup>a</sup>, Clancy W. James<sup>b</sup> and Konstantinos Pikounis<sup>c</sup>  
for the KM3NeT Collaboration**

<sup>a</sup>*Friedrich-Alexander-Universität Erlangen-Nürnberg, Erlangen Centre for Astroparticle Physics,  
Erwin-Rommel-Str. 1, 91058 Erlangen, Germany*

*E-mail: [thomas.heid@fau.de](mailto:thomas.heid@fau.de)*

<sup>b</sup>*Friedrich-Alexander-Universität Erlangen-Nürnberg, Erlangen Centre for Astroparticle Physics,  
Erwin-Rommel-Str. 1, 91058 Erlangen, Germany*

*E-mail: [clancy.james@fau.de](mailto:clancy.james@fau.de)*

<sup>c</sup>*N.C.S.R. Demokritos, Patriarchou Gregoriou and Neapoleos 27, Agia Paraskevi, Greece and  
National Technical University of Athens, Heroon Polytechniou 9, Zografou Campus, Greece*

*E-mail: [pikounis@inp.demokritos.gr](mailto:pikounis@inp.demokritos.gr)*

The main objective of the future neutrino telescope KM3NeT/ARCA is the detection and measurement of high-energy extraterrestrial neutrinos. Atmospheric neutrinos, which are produced in particle showers in the Earth's upper atmosphere, represent the main background to this signal. Muon bundles which accompany down-going atmospheric neutrinos can be used to differentiate the latter from their extraterrestrial counterparts and thus to identify cosmic neutrino signals from the upper hemisphere. The program package CORSIKA has been used for simulating extensive air showers. These particle showers contain many particle types, but the only particle type except neutrinos penetrating the water layer above the detector are muons. A veto strategy against atmospheric neutrinos has been developed which uses the detector signals induced by these muons. In particular these muons modify the observed topology of neutrino-induced events, with a significant effect on different reconstruction parameters. Making use of these effects, most of the downward-going atmospheric neutrinos can be rejected. The corresponding analysis methods and results are reported.

*The 34th International Cosmic Ray Conference,  
30 July- 6 August, 2015  
The Hague, The Netherlands*

## 1. Introduction

KM3NeT aims to detect high-energy astrophysical neutrinos via a gigaton Cherenkov telescope - ARCA - in the Mediterranean Sea. ARCA will comprise two building blocks of 115 vertical strings each. Each string will host 18 Digital Optical Modules (DOMs) to detect the Cherenkov light induced by charged secondary particles from neutrino interactions in the deep sea [1]. One DOM contains 31 photomultiplier tubes (PMTs) covering  $4\pi$  sr [2].

A major source of background is particles originating from cosmic-ray interactions in the upper atmosphere. As the detector is deep in the sea only muons and neutrinos can reach it. A method is presented to suppress neutrinos originating in the atmosphere, making use of the fact that muons accompany many down-going atmospheric neutrinos [3] [4]. This leads to event topologies that can be discriminated from those of unaccompanied, i.e. cosmic neutrinos.

CORSIKA simulates atmospheric air showers. Compared to the expected spectra of atmospheric neutrinos (see Figure 1), the CORSIKA simulations show discrepancies, especially in the upper energy range. The simulated events thus have to be re-weighted according to the known flux at the detector site. Using a preliminary CORSIKA production of atmospheric air showers it is demonstrated how the “self-veto” effect of muons from atmospheric air showers can be used to reduce the background of down-going atmospheric neutrinos by a factor of two in a diffuse flux analysis.

## 2. Simulation codes and analysis

Evaluating the rejection of atmospheric neutrinos requires several simulations. First the standard simulation is described, and afterwards the dedicated CORSIKA simulation of air showers.

### 2.1 Standard simulation in KM3NeT/ARCA

A dedicated program simulates neutrino interactions in the vicinity of the detector. Weights are assigned to the events according to the cross-section and atmospheric neutrino flux. For the latter, the parameterization by Honda et al.[5] is used with the prompt neutrino contribution as described in Enberg et al.[6][6]. A correction factor to these fluxes is applied account for knee in the cosmic ray spectrum [7].

The atmospheric neutrino flux of the standard production is here described by the conventional Honda et al. parametrization [5] with the prompt neutrino contribution from Enberg et al. [6], a correction factor to these fluxes is applied to take care of the Cosmic Ray spectrum knee [7].

Down-going single muons and muon bundles are simulated to study the muon background. Here MUPAGE is used [8]. The muon energy and multiplicity distributions are based on parametrised tables [9].

A further step is the simulation of the detector response. A program called km3 simulates the Cherenkov photons emitted along the path of charged particles involved in the neutrino interactions and detected by ARCA PMTs according to tabulated distributions [10].

The final step is the simulation of the trigger algorithms. In this step the optical background from potassium-40 decays is added [11].

## 2.2 Simulating atmospheric air showers

CORSIKA [12] simulates extensive atmospheric showers initiated by cosmic ray interactions, and is used to produce the air showers for KM3NeT. In this analysis CORSIKA version 7.4001<sup>1</sup> is used. For high-energy hadronic interactions QGSJET01 [13] is used. One restriction is that charmed particles are only produced in their ground states (D+, D-, D0); the effect of this simplification is partially corrected for in Sec. 2.4, but will need further attention in the future.

The primary composition is assumed according to Ref. [14]. It describes the differential flux of primaries from protons up to iron for energies below the knee of the cosmic ray spectrum at around 5 PeV. Above the knee and up to the ankle at  $5 \cdot 10^{18}$ eV the differential flux is extrapolated by reducing the spectral index by 0.3 for every type of primary.

The analysis is based on a production of cosmic rays for zenith angles between  $0^\circ$  and  $87^\circ$ . The events are produced in nine energy regions, ranging from 10 TeV up to 10 EeV. The corresponding event statistics and effective livetimes are summarized in Table 1.

Shower's primary energy range	Number of showers	Livetime (seconds)
10 - 50 TeV	$61.2 \cdot 10^6$	$1.0 \cdot 10^3$
50 - 200 TeV	$41.0 \cdot 10^6$	$1.0 \cdot 10^4$
200 - 1000 TeV	$20.2 \cdot 10^6$	$5.0 \cdot 10^4$
1 - 5 PeV	$2.8 \cdot 10^6$	$1.0 \cdot 10^5$
5 - 20 PeV	$1.6 \cdot 10^6$	$1.0 \cdot 10^6$
20 - 100 PeV	$1.1 \cdot 10^6$	$1.0 \cdot 10^7$
100 - 500 PeV	$4.9 \cdot 10^5$	$1.0 \cdot 10^8$
500 - 2000 PeV	$2.2 \cdot 10^5$	$1.0 \cdot 10^9$
2000 - 10000 PeV	$1.5 \cdot 10^5$	$1.0 \cdot 10^{10}$

Table 1: CORSIKA production statistics.

CORSIKA propagates all particles up to sea level. Additionally, an energy cut is applied to the particles. All muons and neutrinos with less than 10 TeV are discarded, because in a high-energy physics analysis events with less energy would be discarded anyway. Since the goal is to estimate the self-veto effect in a high-energy cascade analysis, only events with muons and neutrinos are kept. For that reason, one neutrino in each event is forced to interact inside the detector, and down-weighted according to the probability for any neutrino to interact [15]. The rest of the neutrinos are discarded.

From this step on, the same steps as in the standard simulation chain are used.

## 2.3 Analysis of simulated neutrino spectra

Figure 1 shows the neutrino spectrum simulated within the standard production and the spectrum produced by the CORSIKA simulation. It can be seen that the spectra differ at energies above  $10^6$  GeV, where the CORSIKA simulation underestimates the neutrino yield by up to a factor of ten. This underestimate is corrected for via the re-weighting procedure in Section 2.4.

<sup>1</sup>In the official version a bug occurs if neutrinos are simulated, and the atmosphere is treated as not planar, which is not accurate for high zenith angles. Unofficial modifications have been introduced to fix this behaviour.

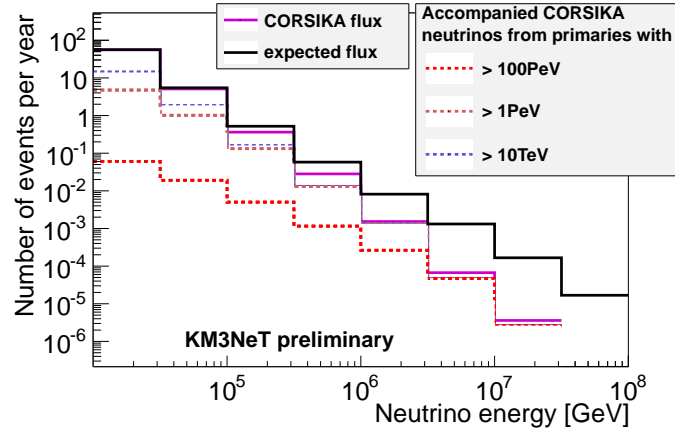


Figure 1: Contributions of different regions of primary cosmic ray energy to the neutrino flux from the CORSIKA simulation, compared to the Honda parameterization for the atmospheric neutrino flux applied to the standard production. All fluxes shown for  $\bar{\nu}_\mu$  of neutral current at trigger level

Primary cosmic particles produce atmospheric neutrinos in different energy regions. In our analysis not every region is of same interest. Figure 1 shows the contributions of different primary energy regions. The diagram shows the simulated flux per year.

The primary cosmic-ray spectrum follows a power law with an index of -2.7, resulting in a neutrino spectrum with an index of -3.7. The most interesting region begins at an energy of  $10^5$  GeV, where the current analysis obtains the highest sensitivity [16]. Cosmic rays of energy 1 PeV to 100 PeV have the largest influence in this region. For current investigations it is important that these primary particles are simulated with high statistics.

#### 2.4 Re-weighting the simulated neutrino flux to the expected neutrino flux

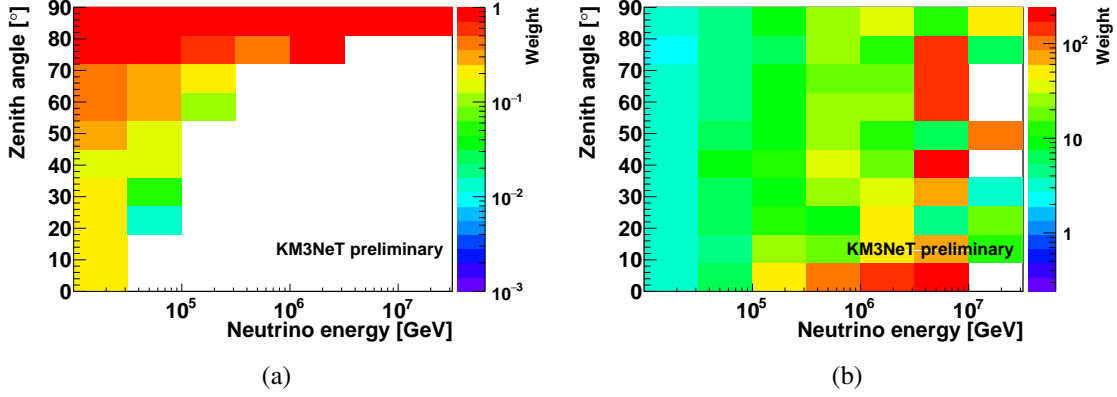
As shown in Figure 1, the expected neutrino spectrum and the simulated neutrino spectrum are different. The aim of re-weighting is to combine the standard neutrino production and the CORSIKA production so that the overall neutrino flux corresponds to the expected neutrino flux described above, and accurately reflects the fraction of accompanied and unaccompanied events.

The spectrum depends on the zenith angle, neutrino energy and flavour, so the weighting has to be a function of these parameters. In the following steps all calculations are made with steps of the size of half a magnitude in neutrino energy and  $9^\circ$  in zenith angle, as the current number of simulated events, in the order of  $10^8$ , does not allow a finer binning.

Further, the re-weighting must be applied separately for each neutrino flavour and interaction type (NC and CC) as flux and event topology is different. In total eight (two flavours, two particle/antiparticle, and charged current/ neutral current) weighting tables are produced.

The final sample of events can be obtained by adding the re-weighted number of CORSIKA events to the re-weighted number of single events. This number will be equal to the expected number at the detector site.

The unaccompanied neutrino flux, for which the standard neutrino production is used, is re-weighted by a factor of  $W_G$  ( $<1$ ) according to the fraction of unaccompanied events in the COR-


 Figure 2: Weights for using the standard (a) and the CORSIKA (b) production for  $\bar{\nu}_e$ -CC

SIKA production. This leads to

$$W_G(\theta, E, \ell, I) = \frac{F_U(\theta, E, \ell, I)}{F_C(\theta, E, \ell, I)}. \quad (2.1)$$

where  $F_U$  is the flux of unaccompanied events simulated by CORSIKA, and  $F_C$  is the total flux of CORSIKA events. The accompanied neutrino flux, simulated with the CORSIKA production, implicitly includes the fraction of accompanied events in its weight, since only these events are considered. However, this production has to be re-weighted so that the total flux of the CORSIKA production is at the level of the standard production. The weight for CORSIKA events is therefore given by

$$W_C(\theta, E, \ell, I) = \frac{F_G(\theta, E, \ell, I)}{F_C(\theta, E, \ell, I)}, \quad (2.2)$$

where  $F_G$  is the flux expected by the standard atmospheric neutrino production.

The only component on which the calculation of weights depends which is subject to significant uncertainties is the expected atmospheric neutrino flux. Weights must be recalculated if it is changed.

Figures 2a and 2b show the final weights used with the appropriate productions. Only weights for anti-electron neutrinos are shown. Figure 2a shows the additional weight to the standard neutrino production. High zenith angles are dominated by neutrino events with no accompanied muons, so the weight is approximately one. At large zenith angles mostly all muons get absorbed or during propagation through the atmosphere or water above the detector. The higher the neutrino energy the higher the probability that muons accompany the neutrino to the detector. In this histogram, empty bins indicate ranges where no neutrino reaches the detector unaccompanied. As the standard production is the reference, neutrino flux weights cannot become larger than one, other than for the weights of the CORSIKA production.

Figure 2b shows the weight  $W_C$  one has to apply to the CORSIKA production. The weights are rather constant along the zenith angle. The trend to larger weights at high energies reflects the afore-mentioned underestimation of neutrinos inside the CORSIKA simulation. Large fluctuations above an energy of  $10^6$  GeV shows a lack of statistics. Furthermore above  $10^7$  GeV the production

is so sparse as to be almost unusable. For the current analysis this is not a significant drawback, because the used energy ranges are mostly between  $10^5$  and  $10^6$  GeV (although in this region there are small fluctuations).

### 2.5 Self-Veto and application to sensitivity

The CORSIKA weights are applied to the sensitivity calculation for the diffuse neutrino flux in KM3NeT. In the following a short overview of the cut-and-count analysis is given. More details can be found in [16].

The analysis looks for high-energy events which are consistent with a cascade-like topology. The analysis is based on a multi-step rejection of atmospheric background. A boosted decision tree [17] is used to discriminate against atmospheric muon events. Accompanying muons will thus cause neutrino cascade events to be rejected on the basis that the event no longer looks cascade-like. The final sensitivity calculation is done with a cut-and-count method as described in [18].

### 3. Results

Figures 3a show the probability that an atmospheric neutrino which is not accompanied by muons survives in the analysis described above. One can see the survival probability is very low at energies below  $10^5$  GeV as this analysis tries to increase the sensitivity to the high-energy signal. The maximum probability of survival of around 50% reflects, that events are simulated all over the can. Many of them are too distant from the detector to be used in the analysis. Figure 3b shows the additional probability to survive (1-chance of being rejected) if the neutrino is accompanied by muons. Events near the horizontal cannot be rejected, as many of the muons do not reach the detector. So the event topology is dominated by neutrinos. By contrast the sample of low zenith angles consists mostly of events dominated by muons. Empty bins symbolise that were no events left before or all events are rejected. Zenith angles up to 50 degrees are suppressed completely.

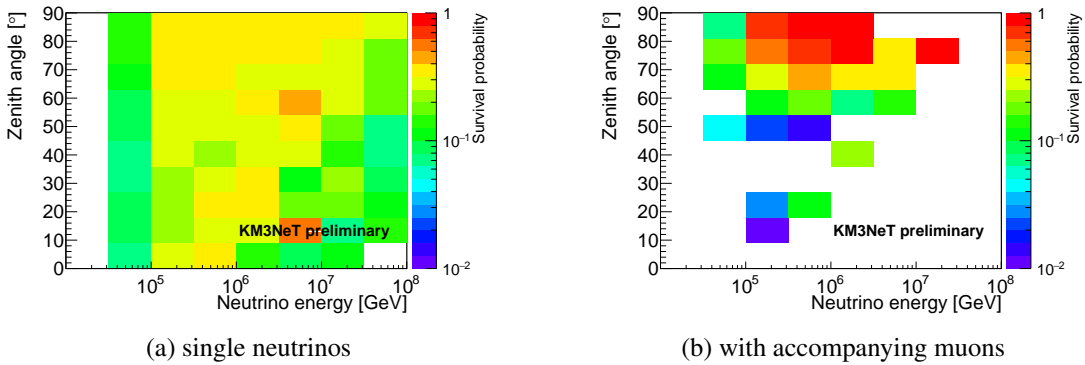


Figure 3: Probability of neutrino events in  $\bar{\nu}_e$ -charged current surviving the final cuts. (a) single neutrinos. (b) additional survival probability for accompanied neutrinos

Figures 4a and 4b show the distribution of expected down-going atmospheric neutrinos as a function of energy, both with and without<sup>2</sup> the self-veto effect. Figure 4 reflects the behaviour of

<sup>2</sup>By setting  $W_C = 0$ ,  $W_G = 1$

Figure 3. Low-energy events are rejected with high probability. Low zenith angles behave the same way, due to the self-veto effect. However, the upper left region between  $10^{4.5}$  GeV and  $10^6$  GeV and at high zenith angles cannot be suppressed as well as other regions.

Applying the cut-and-count method without rejecting CORSIKA events, 1.5 events are left after the final selection in a sample with all neutrino flavours. Applying the new weights and combining CORSIKA events and standard neutrinos the selection leaves 0.7 events in this zenith angle region. The total number of surviving upcoming neutrino events is 1.5 in this analysis. The analysis is supposed to reject atmospheric muons, so more down-going events are rejected. The number of up-going and down-going neutrinos are equal although Earth absorption cause a reduction of up-going events.

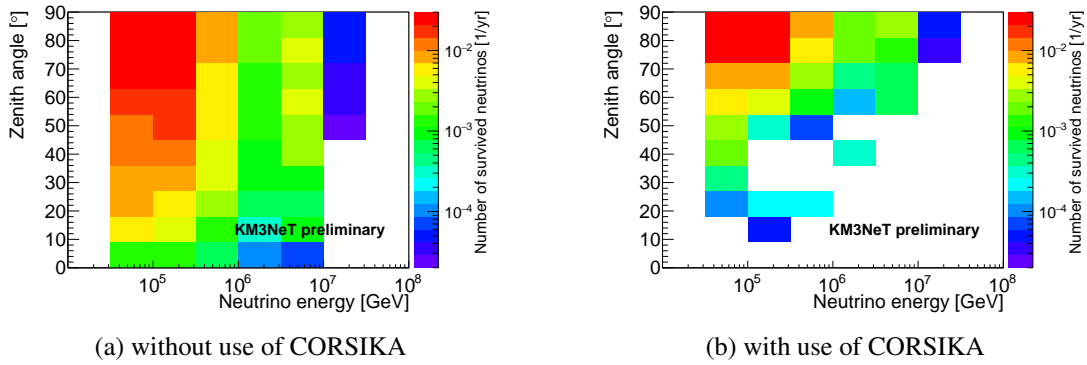


Figure 4: Number of surviving atmospheric neutrinos after selection for the cut-and-count analysis for diffuse neutrino flux in KM3NeT in  $\bar{\nu}_e$ -charged current

#### 4. Conclusion and Perspectives

KM3NeT aims to detect extraterrestrial neutrinos for both point-like searches and diffuse searches. For every study atmospheric muons and neutrinos are an overwhelming background. Here techniques are developed to suppress atmospheric neutrinos. The algorithms can detect them because many of them are accompanied by muons, as they are produced in the upper atmosphere by cosmic rays.

Atmospheric neutrino simulations with CORSIKA do not follow the expected atmospheric neutrino spectrum. Thus the resulting flux of the air shower simulation is re-weighted so that the combination of single neutrinos and accompanied neutrinos corresponds to the expected flux.

The next step in this approach is to fine-tune and use more recent composition models for primary cosmic rays and interaction models for the CORSIKA simulation, and produce a larger sample of events to reduce statistical fluctuations above 1 PeV. An updated CORSIKA production is currently underway.

As proof of concept the application to the diffuse flux search shows that the amount of atmospheric neutrinos could be reduced from 1.5 expected down-going atmospheric neutrinos to 0.7 atmospheric neutrinos. In this analysis we saw for the first time that a full CORSIKA simulation was used through the complete chain.

As all analyses can profit from rejecting atmospheric neutrinos a more general use of this approach is encouraged. It should be noted that this ‘rejection’ can also be used as an ‘identification’ of atmospheric neutrinos, in order to measure the prompt flux.

## References

- [1] P. Piattelli in *these proceedings*.
- [2] R. Bruijn in *these proceedings*.
- [3] S. Schonert et al. *Phys. Rev.* **D79** (2009) 043009.
- [4] T. K. Gaisser et al. *Phys. Rev.* **D90** (2014), no. 2 023009.
- [5] M. Honda et al. *Phys. Rev. D* **75** (2007) 043006.
- [6] R. Enberg et al. *Phys. Rev. D* **78** (2008) 043005.
- [7] M. Aartsen et al. *Phys. Rev. D* **89** (2014) 062007.
- [8] G. Carminati et al. *Computer Physics Communications* **179** (2008), no. 12 915 – 923.
- [9] Y. Becherini et al. *Astroparticle Physics* **25** (2006) 1–13.
- [10] A. Margiotta *Nuclear Instruments and Methods in Physics Research A* **725** (2013) 98–101.
- [11] A. Creusot in *these proceedings*.
- [12] D. Heck et al. *FZKA-6019* (1998).
- [13] N. Kalmykov et al. *Bull. Russ. Acad. Sci. Phys.* **58** (1994) 1966–1969.
- [14] B. Wiebel-Sooth et al. *Astronomy and Astrophysics* **330** (1998) 389–398.
- [15] R. Gandhi et al. *Phys. Rev. D* **58** (1998) 93009. 32 p.
- [16] D. Stransky in *these proceedings*.
- [17] A. Hoecker et al. *PoS ACAT* (2007) 040.
- [18] G. Hill et al. *Astroparticle Physics* **19** (2003), no. 3 393 – 402.